



## LJMU Research Online

**Freeman, SL, Kwon, H, Portolano, N, Parkin, G, Venkatraman Girija, U, Basran, J, Fielding, AJ, Fairall, L, Svistunenko, DA, Moody, PCE, Schwabe, JWR, Kyriacou, CP and Raven, EL**

**Heme binding to human CLOCK affects interactions with the E-box.**

<http://researchonline.ljmu.ac.uk/id/eprint/11419/>

### Article

**Citation** (please note it is advisable to refer to the publisher's version if you intend to cite from this work)

**Freeman, SL, Kwon, H, Portolano, N, Parkin, G, Venkatraman Girija, U, Basran, J, Fielding, AJ, Fairall, L, Svistunenko, DA, Moody, PCE, Schwabe, JWR, Kyriacou, CP and Raven, EL (2019) Heme binding to human CLOCK affects interactions with the E-box. *Proceedings of the National Academy of Sciences***

LJMU has developed [LJMU Research Online](http://researchonline.ljmu.ac.uk/) for users to access the research output of the University more effectively. Copyright © and Moral Rights for the papers on this site are retained by the individual authors and/or other copyright owners. Users may download and/or print one copy of any article(s) in LJMU Research Online to facilitate their private study or for non-commercial research. You may not engage in further distribution of the material or use it for any profit-making activities or any commercial gain.

The version presented here may differ from the published version or from the version of the record. Please see the repository URL above for details on accessing the published version and note that access may require a subscription.

For more information please contact [researchonline@ljmu.ac.uk](mailto:researchonline@ljmu.ac.uk)

<http://researchonline.ljmu.ac.uk/>

## HEME BINDING TO HUMAN CLOCK AFFECTS INTERACTION WITH THE E-BOX

Samuel L Freeman<sup>1</sup>, Hanna Kwon<sup>1</sup>, Nicola Portolano<sup>2</sup>, Gary Parkin<sup>2</sup>, Umakhanth Venkatraman Girija<sup>2,¶</sup>, Jaswir Basran<sup>2</sup>, Alistair J. Fielding<sup>4</sup>, Louise Fairall<sup>3</sup>, Dimitri A. Svistuneko<sup>5</sup>, Peter C. E. Moody<sup>3</sup>, John W. R. Schwabe<sup>3</sup>, Charalambos P. Kyriacou<sup>6</sup> and Emma L. Raven<sup>1,\*</sup>

### AFFILIATIONS

<sup>1</sup> School of Chemistry, University of Bristol, Cantock's Close, Bristol, BS8 1TS, UK

<sup>2</sup> Department of Chemistry and Leicester Institute of Structural and Chemical Biology, University of Leicester, University Road, Leicester, LE1 7RH, UK

<sup>3</sup> Department of Molecular and Cell Biology and Leicester Institute of Structural and Chemical Biology, University of Leicester, University Road, Leicester, LE1 7RH, UK

<sup>4</sup> School of Pharmacy and Biomolecular Science, James Parsons Building, Byrom Street, Liverpool, L3 3AF, England UK

<sup>5</sup> School of Biological Sciences, University of Essex, Wivenhoe Park, Colchester, Essex, CO4 3SQ, England UK

<sup>6</sup> Department of Genetics, Adrian Building, University of Leicester, University Road, LE1 7RH, England UK

¶ Current address: Faculty of Health and Life Sciences, De Montfort University, Leicester, UK

\* To whom correspondence should be addressed. School of Chemistry, University of Bristol, Cantock's Close, Bristol, BS8 1TS, UK. Telephone: +44 (0)117 9287657; E-mail: emma.raven@bristol.ac.uk.

**CLASSIFICATION:** Biological sciences; biochemistry.

### ABSTRACT

The circadian clock is an endogenous time-keeping system that is ubiquitous in animals and plants as well as some bacteria. In mammals, the clock regulates the sleep-wake cycle via two basic helix-loop-helix PER-ARNT-SIM (bHLH-PAS) domain proteins - CLOCK and BMAL1. There is emerging evidence to suggest that heme affects circadian control, through binding of heme to various circadian proteins, but the mechanisms of regulation are largely unknown. In this work we examine the interaction of heme with human CLOCK (hCLOCK). We present a crystal structure for the PAS-A domain of hCLOCK, and we examine heme binding to the PAS-A and PAS-B domains. UV-visible and EPR spectroscopies are consistent with a bis-histidine ligated heme species in solution in the oxidised (ferric) PAS-A protein, and by mutagenesis we identify His144 as a ligand to the heme. There is evidence for flexibility in the heme pocket, which may give rise to an additional Cys axial ligand at 20K (His/Cys coordination). Using DNA binding assays, we demonstrate that heme disrupts binding of CLOCK to its E-box DNA target. Evidence is presented for a conformationally mobile protein framework, which is linked to changes in heme ligation and which has the capacity to affect binding to the E-box. Within the hCLOCK structural framework, this would provide a mechanism for heme-dependent transcriptional regulation.

**KEYWORDS:** Heme, circadian.

### SIGNIFICANCE STATEMENT

Heme proteins have several well-established functions in biology, from oxygen transport to electron transfer and catalysis. But in addition, there is new evidence that heme has a wider regulatory role in the cell. This includes a role for heme in the regulation of circadian rhythm. In this work, we have examined the binding of heme to human CLOCK, one of the positive elements in the circadian autoregulatory feedback loop. We find evidence for a conformational mobility within the heme pocket, and that heme disrupts binding of CLOCK to its E-box DNA. These results provide a direct link between heme binding and DNA partner recognition that may form the basis for a mechanism of regulatory control.

## INTRODUCTION

\body

The circadian clock is the internal timekeeping system that generates a daily rhythm in physiology, biochemistry and behaviour of almost all higher organisms and some prokaryotes. In mammalian systems, as in insects, a transcriptional-translational feedback loop appears to be at the core of the oscillator (1), and this is coupled to an evolutionarily more primitive metabolic oscillator (2). The transcriptional-translational feedback loop has a number of positive and negative components that drive interconnected loops that generate the molecular clockworks. In mammals, NPAS2 (in the forebrain) and CLOCK (in the suprachiasmatic nucleus) form heterodimers with BMAL1 (brain and muscle arnt-like 1) and represent the positive limb of the feedback loop (Fig. 1). Both dimers bind to the same E-box DNA sequence (*CANNTG*) to activate expression of the negative autoregulators, the three Period (*Per*) and two Cryptochrome (*Cry*) genes (1). PER and CRY, after various posttranslational modifications that build delays into the loop, then interact with the BMAL1 complexes to negatively regulate their own genes, thereby closing the loop (Fig. 1 and (1)). REV-ERB $\alpha$ , a member of the nuclear receptor family, also functions in the cell to repress transcription of BMAL1.

There is an accumulating body of evidence that indicates that heme is a regulator of the circadian oscillator (3), but the mechanisms of regulation are entirely unknown. Conceptually, heme binding provides a simple mechanism for signal transduction because regulation by heme can be coupled to its ability to bind other ligands - such as oxygen ( $O_2$ ), carbon monoxide (CO) and nitric oxide (NO) - which are themselves established as important signalling molecules in cellular control (4).

The two E-box binding proteins - NPAS2 and CLOCK - belong to the family of transcriptional regulators that contain both basic helix-loop-helix (bHLH) domains at the N-terminus as well as two PAS domains. High sequence identity between these two proteins (5, 6) was noted before a direct link between heme and any circadian protein had been established. In this work we present an analysis of heme binding to the PAS-A domain of human CLOCK, we examine the effect of heme on the CLOCK-DNA binding interaction, and we present a structure for the PAS-A domain. We use this information to put forward ideas on how heme binding might be linked to regulation of circadian control.

## RESULTS

*Crystal structure of hCLOCK PAS-A.* A recombinant version (N-terminal His-tagged) of the PAS-A domain of hCLOCK (hCLOCK PAS-A, Fig. 2) was expressed in *E. coli*. The purified protein crystallised as a homodimer in the apo-form (*i.e.* without heme), consistent with behavior of the protein during size exclusion chromatography (Fig. S2).

The structure of the hCLOCK PAS-A structure is presented in Fig. 3A. The tertiary structure of the overall PAS fold consists of a series of antiparallel  $\beta$ -sheets forming a hydrophobic core in which a signalling molecule can bind (7). A number of  $\alpha$ -helices are in close proximity which are believed to be responsible for the propagation of structural changes to the rest of the protein or to a partner protein when in a complex.

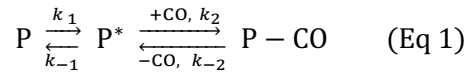
The hCLOCK structure has close similarity to that of the  $O_2$  sensor from *Rhizobium* (FixL, (8)) and the heme-regulated phosphodiesterase from *Escherichia coli* (EcDOS, (9, 10)), as shown in Figs. 3B,C. A comparison of the heme binding locations in the two structures is informative, Fig. S3. In the structure of hCLOCK PAS-A, histidine 144, which is implicated in heme binding as below, is found on a loop between two short helices and is oriented towards the  $\beta$ -sheets of the domain in a hydrophobic pocket. This hydrophobic core is a feasible heme binding pocket, as shown in Fig. S3. From the hCLOCK structure, it appears that H144 is a realistic proximal residue for heme and is ideally situated at the mouth of this hydrophobic pocket and is surrounded by numerous hydrophobic residues (Phe 121, Leu 145, Leu 149, Phe 157 and Leu 198) which leave adequate space for a heme molecule. A comparison with FixL shows that the heme in the crystal structure of FixL is located in a different location, at the opposite end of this hydrophobic pocket, Fig. S3A.

*Heme binding to hCLOCK PAS-A.* Although heme is not present in the structure of hCLOCK above, binding of heme to the PAS-A domain of hCLOCK is clearly evident from UV-visible spectra. The spectrum of the oxidised, ferric derivative of hCLOCK PAS-A ( $\lambda_{\max} = 413, 533$  nm, Fig. 4A) is consistent with heme binding to the protein and with a 6-coordinate, low spin heme species. EPR spectra

are in agreement with this assignment. The spectrum of heme-bound hCLOCK at 20 K (Fig. 4B) reveal turning points at  $g_1 = 2.93$ ,  $g_2 = 2.28$ , and  $g_3 \geq 1.7$  typical of a low-spin, ferric ( $S = 1/2$ ) heme species (11). These low-spin  $g$ -values are consistent with a bis-histidine heme coordination. Weak resonances were also observed at 4 K at  $g^{\text{eff}} \approx 6.0$  and  $g^{\text{eff}} \approx 2$ , which are characteristic of high-spin ferric ( $S = 5/2$ ) heme (Fig. S4A). In addition, a shoulder is observed on the central line and attributed to overlap of a second (minor) low-spin heme species ( $g_3 = 2.45$ ,  $g_2 = 2.28$ , and  $g_3 = 1.92$ ). These  $g$ -values are similar to those previously observed for the isolated PAS-A domain of mouse Per2 (12). Empirical  $g$ -values for heme-bound species are well studied (11). In this case the  $g$ -values for the second species in the EPR are unlike those reported for either His/His or His/Met ligation, and on this basis are assigned as arising from a Cys/His or Cys/OH<sup>-</sup> coordination.

Heme binds to apo-hCLOCK with a 1:1 stoichiometry ( $K_D = 4.2 \pm 0.25 \mu\text{M}$ , Fig. 4A inset). Heme dissociation from hCLOCK PAS-A was measured at 412 nm in the presence of the H64Y/V68F mutant of sperm whale myoglobin which has a high affinity for heme (13) (Fig. 4C). A biphasic exponential change was observed giving rate constants of  $8.9 \times 10^{-3} \text{ s}^{-1}$  and  $4.5 \times 10^{-4} \text{ s}^{-1}$  for the fast and slow phases respectively. This biphasic behaviour is consistent with the concept of conformational mobility within the heme binding site. The rate constants for heme dissociation are consistent with those derived for other heme regulatory such as SOUL and p22HBP ( $k_{\text{diss}} \approx 10^{-3} \text{ s}^{-1}$  (14)).

As for the ferric protein above, the ferrous derivative of hCLOCK PAS-A ( $\lambda_{\text{max}} = 425, 533$  and  $558 \text{ nm}$ , Fig. 4D), shows characteristic heme peaks, which is again consistent with 6-coordinate, low spin heme. On the basis of similarities to ferrous NPAS2 ( $\lambda_{\text{max}} = 423, 530$  and  $558 \text{ nm}$  (15)), which is assigned as a His/His ligated heme species (16), we assign hCLOCK PAS-A as the same. Ferrous hCLOCK binds both CO ( $\lambda_{\text{max}} = 421, 540$  and  $570 \text{ nm}$ , Fig. 4D) and NO ( $\lambda_{\text{max}} = 421, 531$  and  $556 \text{ nm}$ , Fig. 4D), with a presumed His/CO ligation. In kinetic experiments measuring CO binding to hCLOCK PAS-A, pseudo-first order rate constants ( $k_{\text{obs}}$ ) showed a non-linear dependence on the concentration of CO, but were linearly dependent on the protein concentration, Fig. 4E. This kinetic behaviour is consistent with a dynamic equilibrium of the protein structure (P) prior to CO binding (17), presumably leading to loss of one of the axial His ligands, eq [1],



and in the case where CO binding is irreversible ( $k_{-2} \ll k_1 k_2 / k_{-1}$ ) a hyperbolic dependence of  $k_{\text{obs}}$  on CO concentration is observed, eq. [2].

$$k_{\text{obs}} = k_1 k_2 [\text{CO}] / (k_{-1} + k_2 [\text{CO}]) \quad (\text{Eq 2})$$

The addition of oxygen to ferrous protein under anaerobic conditions gave no evidence of a ferrous-oxy intermediate – this might be linked to the low reduction potential of the heme in hCLOCK PAS-A, which has been previously determined (18, 19) as  $-111 \text{ mV vs NHE}$ .

Based on a sequence alignment with NPAS2, Fig. S5, we identified His144 as a possible ligand to the heme in hCLOCK (equivalent to the axial His119 ligand in NPAS2). The corresponding spectra of the ferric H144A mutant of hCLOCK PAS-A in the presence of heme showed a broad, strongly blue-shifted Soret band ( $\lambda_{\text{max}} = 374 \text{ nm}$ ) which is different from that of the ferric wild-type protein and which is not consistent with a *bona fide* heme protein, Fig. 4F. On this basis, we assign His144 as one of heme ligands in hCLOCK. EPR spectra confirm this assignment as the  $g_1 = 2.93$  resonance is missing in the spectrum of the H144A variant, Fig. 4B. The identity of the proposed Cys ligand seen only at low temperature in the EPR (above) was not established. The most likely candidate was considered to be Cys195 which points towards the heme pocket, but the EPR spectrum of the C195A variant (which corresponds to Cys170 in NPAS2 and has been suggested as a ligand (20)) was unchanged from that of the wild type protein, Fig. 4B. The uv-visible spectrum of the C195A variant is also very similar to the wild type, Fig. S4B, and thiol-modification of apo-hCLOCK with DTNB (to modify all Cys residues) followed by reconstitution with heme did not lead to a change in the uv-visible spectrum. Mutation of the adjacent Cys194 residue gave a similar heme-bound spectrum ( $\lambda_{\text{max}} = 414 \text{ nm}$ ) and was presumed to bind heme normally in solution by virtue of the His144 ligand. Together, we interpret this information to mean that the Cys-ligated species is only present at low (cryogenic) temperatures.

We also expressed a PAS-B fragment of hCLOCK, Figs. 2 and S1, which was found to bind heme in the ferric form ( $\lambda_{\max} = 416$  and  $536$  nm, Fig. S6) but with marginally weaker affinity ( $K_D = 13.3 \pm 0.97$   $\mu\text{M}$ , Fig. S6) than the PAS-A form of hCLOCK. The PAS-B domain of NPAS2 is also reported as binding heme more weakly than the corresponding PAS-A domain (21) but the functional consequences, if any, of this difference are not known because the role of PAS-B is not yet established. The ferrous ( $\lambda_{\max} = 424, 532$  and  $559$  nm, Fig. S6) and CO-bound forms ( $\lambda_{\max} = 421, 541$  and  $569$  nm, Fig. S6) also form normally. Like the hCLOCK PAS-A domain, these spectra are indicative of a 6-coordinate heme binding interaction but this was not examined further in this work.

*Heme affects binding to the E-box.* To assess the functional effect of heme on DNA binding, we expressed a construct of hCLOCK PAS-A containing an N-terminal HLH domain, Fig. 2 and Fig. S7A. The hCLOCK HLH-PAS-A construct was demonstrated to bind to E-box DNA (Fig. 5A); a plot of the relative band intensity versus [hCLOCK HLH/PAS-A] gave a  $K_D = 6.3$   $\mu\text{M}$ , which is similar to that determined ( $K_D = 9$   $\mu\text{M}$ ) for a different construct of CLOCK containing only the HLH domain (22). Control experiments (Fig. 5B) with the corresponding HLH/PAS-A construct of NPAS2 (Fig. S7B and Fig. S8) similarly demonstrated binding of NPAS2 to E-box ( $K_D = 11$   $\mu\text{M}$ , Fig. 5B). These HLH-PAS-A proteins are presumed to bind to DNA as homodimers, as HLH domains are unable to form a specific interaction with E-box DNA in the monomeric form [13].

Addition of heme inhibits DNA binding to the HLH domain of hCLOCK, as evidenced by the shift in the DNA band in EMSA assays, Fig. 5C; the same effect is observed for NPAS2, Fig. 5D. From the intensities of the DNA-protein and the free DNA bands, an  $\text{IC}_{50}$  of  $7.4$   $\mu\text{M}$  was derived for the inhibitory effect of heme on DNA binding to hCLOCK; this value is in the same range as the  $K_D$  for heme binding to the PAS-A domain ( $K_D = 3.7$   $\mu\text{M}$ , above).

## DISCUSSION

*The role of heme in circadian regulation.* In addition to known roles as a prosthetic group in a multitude of heme proteins and enzymes, there is now emerging evidence that heme has a wider role to play in biology. A regulatory mechanism in cells that is linked to heme binding is, to our way of thinking, chemically logical and potentially versatile. Heme is redox active and, thus, responds to redox changes within the cell by modulating its oxidation state. Concentrations of heme in the cell are controlled by the balance of heme biosynthesis (to increase heme concentrations) and heme oxygenase activity (which degrades heme and produces CO as a by-product). Cell-signalling gases ( $\text{O}_2$ , NO and CO) all bind to heme, which creates a possible mechanism of regulatory control. CO is itself produced by degradation of heme by the  $\text{O}_2$ -dependent heme oxygenase enzyme, and NO is produced by the  $\text{O}_2$ -dependent NO synthase enzyme. When one considers this in the context of circadian control, this means that the redox state of the cell, the oxidation state of heme, the balance between heme synthesis and degradation, and  $\text{O}_2/\text{NO}/\text{CO}$  concentrations may all be inter-connected. This is summarised in outline form in Fig. 1. This interconnectivity could form the basis for a powerful heme-dependent circadian control mechanism that reflects metabolic activity. The fact that transcription of ALAS1, the first enzyme in the heme synthesis pathway, and other genes involved in heme catabolism (such as heme oxygenase) and heme transport (23-29) are also clock regulated is also significant as a means of connecting heme synthesis, heme degradation and CO formation to circadian events. Indeed, it has previously been shown that heme-related genes in mouse are also implicated in the light resetting of the clock either as cause or effect (30).

In the case of particular circadian proteins, several – including REV-ERB, PER2, NPAS2 – are shown to bind heme (12, 15, 20, 21, 31-40) and complex formation with partner proteins can be affected by heme or CO binding (34, 41, 42). And there are precedents for a circadian control mechanism that occurs through binding to PAS domain proteins, because of other regulatory PAS domain proteins that are known to bind heme (for example FixL in the histidine kinase family, the phosphodiesterases *EcDOS* and *PDEA1* (43) and *Burkholderia xenovorans* RcoM (16)).

*Structure and heme ligation in hCLOCK.* We have presented a structure for the PAS-A domain of hCLOCK. Heme is not bound to hCLOCK in this structure, although there is convincing evidence for non-covalent heme binding in the UV-visible and EPR spectra, as well as from the kinetic data. The absence of heme in our crystal structure does not imply a lack of specific heme binding - it may be that the particular conformation in which hCLOCK PAS-A crystallises is not compatible with heme binding

correctly in the cavity and thus heme is excluded during crystal formation. An absence of heme in the structure of a presumed heme binding protein has also been noted in the periplasmic heme transporter protein BhuT (44); this has been attributed to structural flexibility of the transporter complex.

Heme binds relatively weakly to the PAS-A domain of hCLOCK, and weak heme binding is a feature of a number of regulatory heme binding proteins (20). The heme is proposed to reside at the mouth of a hydrophobic cavity comprising residues Phe 121, Leu 145, Leu 149, Phe 157 and Leu 198, Fig. S3. This is plausible in the sense that FixL also binds heme in a hydrophobic pocket (residues Val 188, Met 192, Tyr 203, and Ile 204) that helps to orient the heme and the His ligand (His200) in the correct location (8). Our comparison of the structures, Fig. S3, indicates that the heme binds at different locations in hCLOCK and FixL – both locations appear to be viable but the biological relevance of these differences is not yet known.

From the available spectroscopic data for hCLOCK we assign the heme binding interaction in ferric hCLOCK as histidine-ligated at room temperature in solution. Data for the His144 variant strongly implicate this residue as a one of the heme ligands, and His144 is essential for heme binding. The hCLOCK protein appears to contain 6-coordinated (His/His) heme as evidenced by EPR, but appears able to adopt other distinct states with the axial ligand(s) being labile. The identity of the second histidine ligand is not known. There is evidence for a 5-coordinated ferric high-spin heme species from the EPR, again consistent with axial ligand lability (but His144 is presumed not to be labile, as it is essential for heme binding). These data are in agreement with those for NPAS2, which assign the equivalent residue (His119) as an axial ligand (20), Fig. S5. There is evidence from EPR only (empirical interpretation of the EPR g-values) for an additional Cys ligand to the heme in hCLOCK at 20 K. Cys ligation has been suggested in other heme regulatory proteins (16), but the spectroscopic evidence for it in the case of NPAS2 (where Cys170 has been proposed as a ligand, equivalent to Cys195 in hCLOCK, Fig. S5), and particularly in mPer2, is not totally conclusive. In the case of NPAS2, axial ligation might be affected by the presence of the N-terminal HLH domain (12, 20, 45). For hCLOCK, there are three Cys residues in the sequence and one of these (Cys250) is at  $>20 \text{ \AA}$  from His144. Cys195 points towards the pocket, but is still at  $>10 \text{ \AA}$  from the His144 ligand. The adjacent Cys194 residue is exposed and pointing away from the proposed heme pocket. A homology model of hCLOCK and NPAS2, Fig. 6, indicates an overlay of the His144/His119 and Cys195/Cys170 residues. From the evidence available so far, our conclusions are that the axial ligand identities in hCLOCK – and, by analogy, in other related regulatory proteins – are not as straightforwardly defined as in other well-known heme proteins such as myoglobin (His/H<sub>2</sub>O), cytochrome *b*<sub>5</sub> (His/His), cytochrome *c* peroxidase (His/H<sub>2</sub>O) or cytochrome P450 (Cys/H<sub>2</sub>O) which have more rigidly coordinated heme ligands. Instead, we envisage these regulatory heme proteins as being much more fluid in their heme binding – and thus able to change their axial ligation in response to different stimuli, which could be binding to a protein partner, to DNA, to another heme ligand (such as CO) or to a change in oxidation state (16). This would require a degree of flexibility in the heme pocket which, in the case of the CLOCK protein, is consistent with the fact that PAS domains are known to be conformationally mobile (46). We have good evidence for conformational mobility of hCLOCK in our observations, namely the weak heme binding, the absence of heme in the crystal structure, and the required loss of the axial His ligand on CO binding to the ferrous form. This type of protein flexibility has been noted in other regulatory proteins (47) as well as in heme-based sensors (48), and could be a common feature of the way that these regulatory heme proteins operate. Further structural information will be important in resolving these questions.

*Effect of heme on DNA binding and functional implications.* Our data demonstrate that heme inhibits binding of hCLOCK to DNA. This provides evidence for an influence of heme on the DNA binding ability of CLOCK in cells. How might this work and how might it affect signal transduction? We offer the following comments. If the proteins are conformationally mobile, for which there is evidence (as above), then it is plausible that heme binding to the PAS domain causes structural rearrangements that are transmitted and affect the interaction with the E-box. Based on the weak heme binding affinity, it is feasible that the heme binding event is itself reversible; reversible loss of heme has been noted in other systems recently (49) and could contribute to the regulatory control. The PAS domains that have been studied appear to initiate signalling from the central  $\beta$ -sheet region of the structure (50); the signal is then often propagated to the C <sub>$\alpha$</sub>  helix of the PAS domain. His144, which binds to the heme in hCLOCK, is located on the C <sub>$\alpha$</sub>  helix and conformational changes linked to heme binding in this proposed signalling region would therefore provide a convenient mechanism for signal transduction. Binding of signalling gases to the heme (such as CO) might also lead to structural rearrangements in the heme pocket, and

there is evidence for this in the related FixL sensor protein (51). How these signals are further propagated is not yet known.

## MATERIALS AND METHODS

Detailed methods on the following subjects are available in SI Materials and Methods: cloning and mutagenesis, expression and purification, electronic spectroscopy, crystallisation, kinetic measurements, electrophoretic mobility shift assays.

**Author contributions** – P.C.E.M., C.P.K., J.W.R.S., and E.L.R designed the research; S.L.F., H. K., N.P., G.P., U.V.G., J. B., A.J.F., L.F., and D.A.S. performed the experiments; all authors analysed and interpreted data; E.L.R wrote the paper with contributions from all authors.

**Acknowledgements** – We are grateful to the late Dr X. Yang (University of Leicester PROTEX cloning facility) for providing the expression constructs used for this work and Dr J Olson (Rice University) for providing us with apo-H64Y/V68F SwMb. We thank Toru Shimizu for sharing unpublished spectra on NPAS2. This work was funded by BBSRC (grant BB/L006626/1 to ER). We thank the National EPSRC EPR service and Facility for support (NS/A000055/1); and Louise Bird and Raymond Owens (OPPF, Harwell) for help with cloning.

**Competing financial interests.** The authors declare no competing financial interests.

## Supplementary information.

Materials and Methods

Figure S1

Figure S2

Figure S3

Figure S4

Figure S5

Figure S6

Figure S7

Figure S8

Table S1

## References

1. Gallego M & Virshup DM (2007) Post-translational modifications regulate the ticking of the circadian clock. *Nature reviews. Molecular cell biology* 8(2):139-148.
2. Edgar RS, *et al.* (2012) Peroxiredoxins are conserved markers of circadian rhythms. *Nature* 485(7399):459-464.
3. Shimizu T, *et al.* (2015) Gaseous O<sub>2</sub>, NO, and CO in signal transduction: structure and function relationships of heme-based gas sensors and heme-redox sensors. *Chemical reviews* 115(13):6491-6533.
4. Verma A, Hirsch DJ, Glatt CE, Ronnett GV, & Snyder SH (1993) Carbon monoxide: a putative neural messenger. *Science* 259(5093):381-384.
5. King DP, *et al.* (1997) Positional cloning of the mouse circadian clock gene. *Cell* 89(4):641-653.
6. Vitaterna MH, *et al.* (1994) Mutagenesis and mapping of a mouse gene, Clock, essential for circadian behavior. *Science* 264(5159):719-725.
7. Taylor BL & Zhulin IB (1999) PAS domains: internal sensors of oxygen, redox potential, and light. *Microbiology and molecular biology reviews : MMBR* 63(2):479-506.
8. Gong W, *et al.* (1998) Structure of a biological oxygen sensor: a new mechanism for heme-driven signal transduction. *Proc Natl Acad Sci U S A* 95(26):15177-15182.
9. Kurokawa H, *et al.* (2004) A redox-controlled molecular switch revealed by the crystal structure of a bacterial heme PAS sensor. *J Biol Chem* 279(19):20186-20193.
10. Park H, Suquet C, Satterlee JD, & Kang C (2004) Insights into signal transduction involving PAS domain oxygen-sensing heme proteins from the X-ray crystal structure of Escherichia coli Dos heme domain (Ec DosH). *Biochemistry* 43(10):2738-2746.

11. Walker FA (1999) Magnetic spectroscopic (EPR, ESEEM, Mossbauer, MCD and NMR) studies of low-spin ferriheme centers and their corresponding heme proteins. *Coord Chem Rev* 185-6:471-534.
12. Kitanishi K, *et al.* (2008) Heme-binding characteristics of the isolated PAS-A domain of mouse Per2, a transcriptional regulatory factor associated with circadian rhythms. *Biochemistry* 47(23):6157-6168.
13. Hargrove MS, *et al.* (1994) His64(E7)-->Tyr apomyoglobin as a reagent for measuring rates of heme dissociation. *J Biol Chem* 269(6):4207-4214.
14. Sato E, *et al.* (2004) SOUL in mouse eyes is a new hexameric heme-binding protein with characteristic optical absorption, resonance Raman spectral, and heme-binding properties. *Biochemistry* 43(44):14189-14198.
15. Mukaiyama Y, *et al.* (2006) Spectroscopic and DNA-binding characterization of the isolated heme-bound basic helix-loop-helix-PAS-A domain of neuronal PAS protein 2 (NPAS2), a transcription activator protein associated with circadian rhythms. *FEBS J* 273(11):2528-2539.
16. Smith AT, *et al.* (2015) Functional divergence of heme-thiolate proteins: a classification based on spectroscopic attributes. *Chemical reviews* 115(7):2532-2558.
17. Badyal SK, *et al.* (2006) Conformational mobility in the active site of a heme peroxidase. *J Biol Chem* 281(34):24512-24520.
18. Efimov I, *et al.* (2007) The redox properties of ascorbate peroxidase. *Biochemistry* 46(27):8017-8023.
19. Efimov I, *et al.* (2014) A simple method for the determination of reduction potentials in heme proteins. *FEBS letters* 588(5):701-704.
20. Uchida T, *et al.* (2005) CO-dependent activity-controlling mechanism of heme-containing CO-sensor protein, neuronal PAS domain protein 2. *J Biol Chem* 280(22):21358-21368.
21. Koudo R, *et al.* (2005) Spectroscopic characterization of the isolated heme-bound PAS-B domain of neuronal PAS domain protein 2 associated with circadian rhythms. *FEBS J* 272(16):4153-4162.
22. Wang Z, Wu Y, Li L, & Su XD (2013) Intermolecular recognition revealed by the complex structure of human CLOCK-BMAL1 basic helix-loop-helix domains with E-box DNA. *Cell Res* 23(2):213-224.
23. Kaasik K & Lee CC (2004) Reciprocal regulation of haem biosynthesis and the circadian clock in mammals. *Nature* 430(6998):467-471.
24. Guenther CJ, Bickar D, & Harrington ME (2009) Heme reversibly damps PERIOD2 rhythms in mouse suprachiasmatic nucleus explants. *Neuroscience* 164(2):832-841.
25. Ceriani MF, *et al.* (2002) Genome-wide expression analysis in *Drosophila* reveals genes controlling circadian behavior. *The Journal of neuroscience : the official journal of the Society for Neuroscience* 22(21):9305-9319.
26. Panda S, *et al.* (2002) Coordinated transcription of key pathways in the mouse by the circadian clock. *Cell* 109(3):307-320.
27. Zheng B, *et al.* (2001) Nonredundant roles of the mPer1 and mPer2 genes in the mammalian circadian clock. *Cell* 105(5):683-694.
28. Damulewicz M, Loboda A, Jozkowicz A, Dulak J, & Pyza E (2017) Interactions Between the Circadian Clock and Heme Oxygenase in the Retina of *Drosophila melanogaster*. *Mol Neurobiol* 54(7):4953-4962.
29. Mandilaras K & Missirlis F (2012) Genes for iron metabolism influence circadian rhythms in *Drosophila melanogaster*. *Metallomics : integrated biometal science* 4(9):928-936.
30. Ben-Shlomo R, *et al.* (2005) Light pulse-induced heme and iron-associated transcripts in mouse brain: a microarray analysis. *Chronobiology international* 22(3):455-471.
31. Yin L, *et al.* (2007) Rev-erbalpha, a heme sensor that coordinates metabolic and circadian pathways. *Science* 318(5857):1786-1789.
32. Raghuram S, *et al.* (2007) Identification of heme as the ligand for the orphan nuclear receptors REV-ERBalpha and REV-ERBbeta. *Nat Struct Mol Biol* 14(12):1207-1213.
33. Lukat-Rodgers GS, Correia C, Botuyan MV, Mer G, & Rodgers KR (2010) Heme-based sensing by the mammalian circadian protein CLOCK. *Inorg Chem* 49(14):6349-6365.
34. Dioum EM, *et al.* (2002) NPAS2: a gas-responsive transcription factor. *Science* 298(5602):2385-2387.
35. Shimizu T (2012) Binding of cysteine thiolate to the Fe(III) heme complex is critical for the function of heme sensor proteins. *J Inorg Biochem* 108:171-177.

36. Airola MV, Du J, Dawson JH, & Crane BR (2010) Heme binding to the Mammalian circadian clock protein period 2 is nonspecific. *Biochemistry* 49(20):4327-4338.
37. Ishida M, Ueha T, & Sagami I (2008) Effects of mutations in the heme domain on the transcriptional activity and DNA-binding activity of NPAS2. *Biochem Biophys Res Commun* 368(2):292-297.
38. Carter EL, Ramirez Y, & Ragsdale SW (2017) The heme-regulatory motif of nuclear receptor Rev-erb $\beta$  is a key mediator of heme and redox signaling in circadian rhythm maintenance and metabolism. *J Biol Chem* 292(27):11280-11299.
39. Carter EL, Gupta N, & Ragsdale SW (2016) High Affinity Heme Binding to a Heme Regulatory Motif on the Nuclear Receptor Rev-erb $\beta$  Leads to Its Degradation and Indirectly Regulates Its Interaction with Nuclear Receptor Corepressor. *J Biol Chem* 291(5):2196-2222.
40. Minegishi S, Sagami I, Negi S, Kano K, & Kitagishi H (2018) Circadian clock disruption by selective removal of endogenous carbon monoxide. *Sci Rep* 8(1):11996.
41. Masri S, Zocchi L, Katada S, Mora E, & Sassone-Corsi P (2012) The circadian clock transcriptional complex: metabolic feedback intersects with epigenetic control. *Annals of the New York Academy of Sciences* 1264(1):103-109.
42. Klemz R, *et al.* (2017) Reciprocal regulation of carbon monoxide metabolism and the circadian clock. *Nat Struct Mol Biol* 24(1):15-22.
43. Gilles-Gonzalez MA & Gonzalez G (2005) Heme-based sensors: defining characteristics, recent developments, and regulatory hypotheses. *J Inorg Biochem* 99(1):1-22.
44. Naoe Y, *et al.* (2016) Crystal structure of bacterial haem importer complex in the inward-facing conformation. *Nat Commun* 7:13411.
45. Uchida T, Sagami I, Shimizu T, Ishimori K, & Kitagawa T (2012) Effects of the bHLH domain on axial coordination of heme in the PAS-A domain of neuronal PAS domain protein 2 (NPAS2): conversion from His119/Cys170 coordination to His119/His171 coordination. *J Inorg Biochem* 108:188-195.
46. Vreede J, van der Horst MA, Hellingwerf KJ, Crielaard W, & van Aalten DM (2003) PAS domains. Common structure and common flexibility. *J Biol Chem* 278(20):18434-18439.
47. Kobayashi K, *et al.* (2016) Redox-Dependent Dynamics in Heme-Bound Bacterial Iron Response Regulator (Irr) Protein. *Biochemistry* 55(29):4047-4054.
48. Sasakura Y, Yoshimura-Suzuki T, Kurokawa H, & Shimizu T (2006) Structure-function relationships of EcDOS, a heme-regulated phosphodiesterase from *Escherichia coli*. *Accounts Chem Res* 39(1):37-43.
49. Nelp MT, *et al.* (2018) Immune-modulating enzyme indoleamine 2,3-dioxygenase is effectively inhibited by targeting its apo-form. *Proc Natl Acad Sci U S A* 115(13):3249-3254.
50. Moglich A, Ayers RA, & Moffat K (2009) Structure and signaling mechanism of Per-ARNT-Sim domains. *Structure* 17(10):1282-1294.
51. Key J & Moffat K (2005) Crystal structures of deoxy and CO-bound bFixLH reveal details of ligand recognition and signaling. *Biochemistry* 44(12):4627-4635.
52. Claudel T, Cretenet G, Saumet A, & Gachon F (2007) Crosstalk between xenobiotics metabolism and circadian clock. *FEBS letters* 581(19):3626-3633.
53. Huang N, *et al.* (2012) Crystal structure of the heterodimeric CLOCK:BMAL1 transcriptional activator complex. *Science* 337(6091):189-194.
54. Waterhouse A, *et al.* (2018) SWISS-MODEL: homology modelling of protein structures and complexes. *Nucleic acids research* 46(W1):W296-W303.
55. DeLano WL (2002) The PyMOL Molecular Graphics System. *DeLano Scientific, San Carlos, CA, USA*.

## FIGURE LEGENDS

**Figure 1.** Simplified figure of mammalian regulatory clockworks (adapted from (52)). In the positive loop, NPAS2 (dark blue circle) and CLOCK (ditto) form heterodimers with BMAL1 (light blue) which bind to E-box to activate expression of PER (black) and CRY (orange). PER and CRY heterodimers then interact with the BMAL1 heterodimers to negatively regulate their own genes, thereby closing the loop (1). Other CLOCK-related genes are expressed, including the nuclear receptors REV-ERB $\alpha/\beta$  (green) and the retinoid receptor orphan receptor (ROR, pink). ALAS, which controls the synthesis (and hence the concentrations) of heme, is also clock-regulated. See introductory text for details.

**Figure 2.** Domain structure in hCLOCK, showing the N-terminal HLH domains and the two PAS domains (PAS-A, PAS-B). The protein constructs used in this work are also shown. The vectors used for each construct design are shown in Fig. S1.

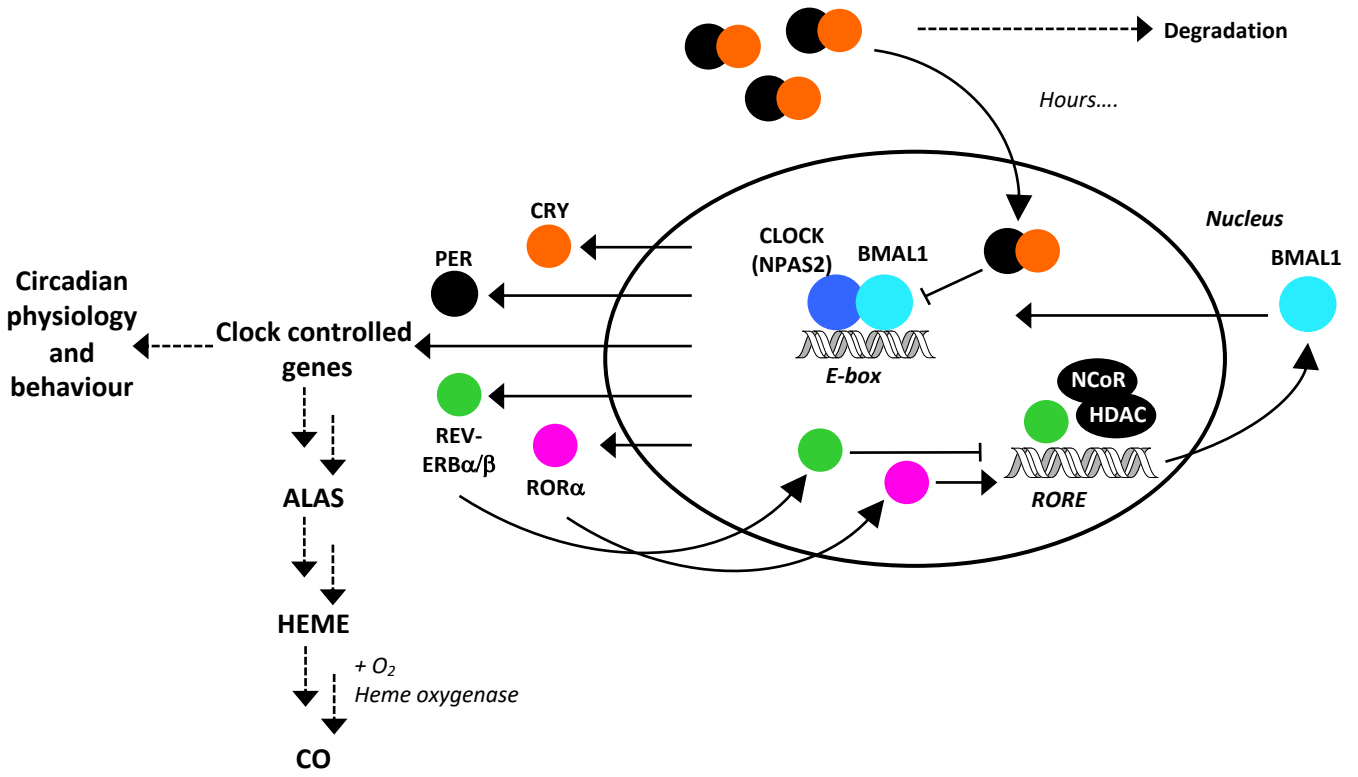
**Figure 3.** A comparison of the structure of PAS-A domains. (A) hCLOCK as presented in this work (PDB code 6QPJ). His144 is indicated in red. This is similar to the equivalent PAS-A domain of mouse CLOCK protein in the CLOCK:BMAL1 complex (53). (B) The O<sub>2</sub> sensor protein from *Rhizobium* (FixL (8)). (C) The heme-regulated phosphodiesterase from *Escherichia coli* (EcDOS, (9, 10)). In (A), and for mouse CLOCK, the protein crystallises in the apo-form. In (B) and (C), which both crystallise as the holo-protein, the heme molecule is indicated in red. The upper figures highlight the binding pocket created by the  $\beta$ -sheets; the lower structures (which are rotated by 90° about the indicated axis) show the similarity in overall arrangement of the domains. For direct comparison, an overlay of the hCLOCK and FixL structures is presented in Fig. S3.

**Figure 4.** (A) UV-Visible absorption spectra of the ferric heme/CLOCK PAS-A complex. Inset shows  $\Delta$ Abs at 415nm (obtained from difference spectra at various heme concentrations) as a function of heme concentration and fitted to a 1:1 binding event. (B) 9 GHz EPR spectra of ferric heme bound to hCLOCK PAS-A (top), the H144A variant of PAS-A (middle) and the C195A variant of PAS-A (bottom) in 50 mM Tris/HCl buffer at pH 7.0. (C) Absorbance change at 412 nm for the dissociation of heme from hCLOCK PAS-A (3-4  $\mu$ M) on mixing with apo-H64Y/V68F myoglobin (80  $\mu$ M). Data are fitted to a double exponential process. (D) Spectrum of the ferrous (solid line), CO-bound (dotted line) and NO-bound (dashed line) derivatives of heme-bound hCLOCK PAS-A. (E) Observed rate constants for the association of CO with hCLOCK PAS-A, shown as a function of [CO] (top) and [hCLOCK PAS-A] (bottom). (F) Spectrum of the ferric heme/CLOCK PAS-A H144A complex (solid line) compared to free ferric heme (dotted line). This spectrum resembles that of the related His335 variant of NPAS2 PAS-B (where H335 is assigned as one of the heme ligands) (21).

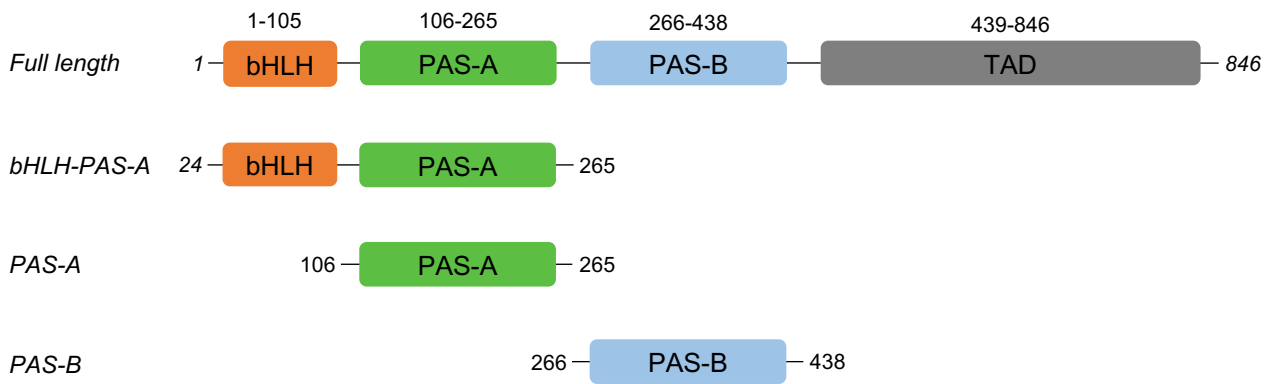
**Figure 5.** Electrophoretic Mobility Shift Assays showing DNA binding to the HLH-PAS-A domains of hCLOCK (A, C) and NPAS2 (B, D) in the absence (A,B) and presence (C,D) of heme.

**Figure 6.** The hCLOCK PAS-A crystal structure as presented in this work (in pale blue, PDB code 6QPJ) superimposed on to a homology model of the PAS-A domain of NPAS-2 (in light grey). Cys195 (equivalent to Cys171 in NPAS2, overlaid in grey) and Cys194 (equivalent to Tyr169 in NPAS2, not shown) in hCLOCK are shown in yellow; Cys250 in hCLOCK is also shown. His144 in hCLOCK is highlighted in red, overlaid with His119 in NPAS2 (in grey). The homology model was produced using SWISS-MODEL (Biozentrum, University of Basel) using the PAS-A domain of the mouse CLOCK structure (PDB code 4F3L) (54). The figure was created using Pymol (55).

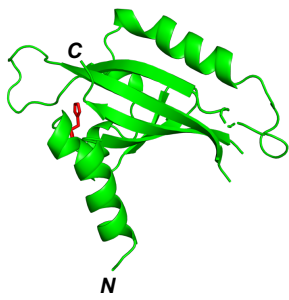
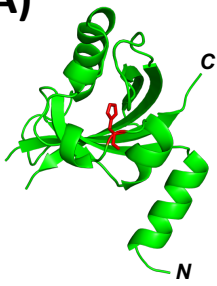
Figure 1 Freeman *et al*



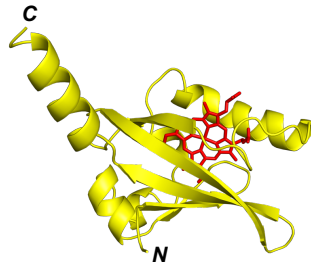
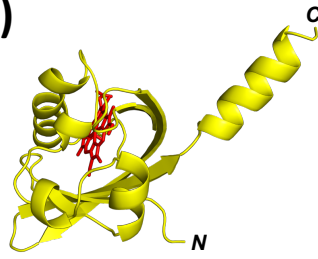
## Human CLOCK



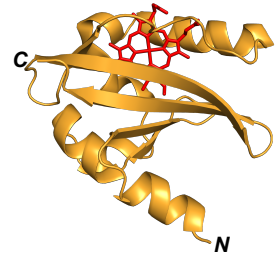
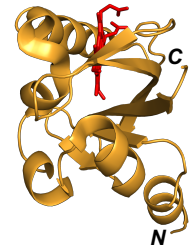
(A)

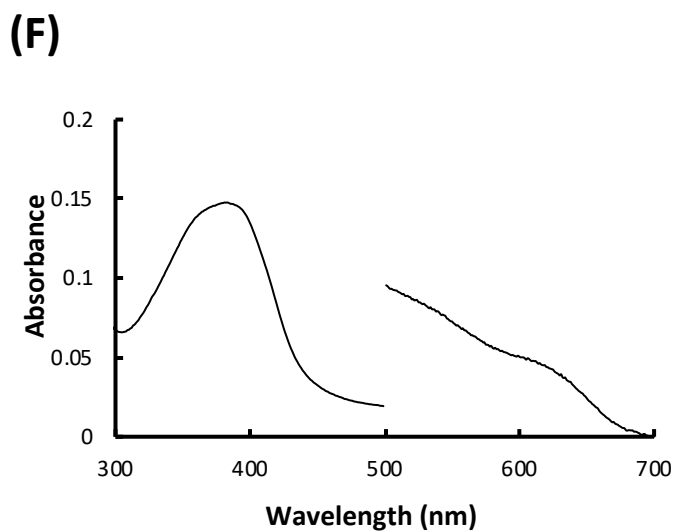
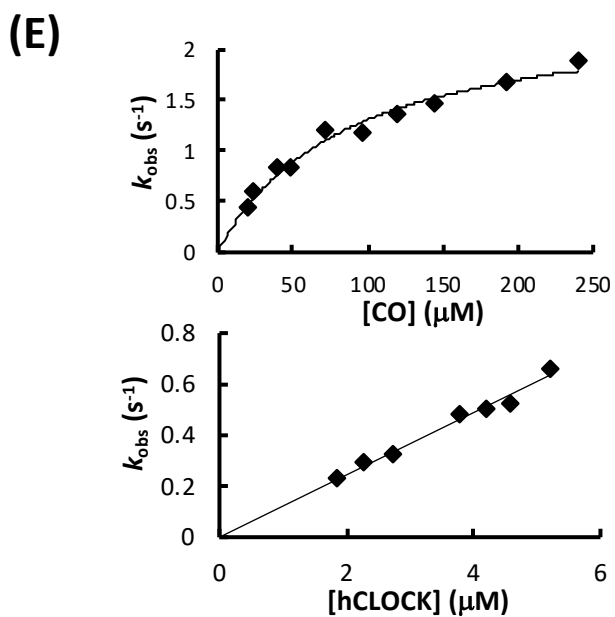
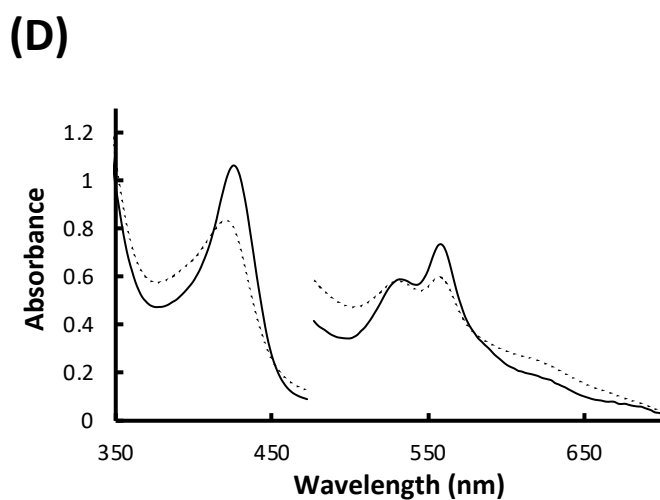
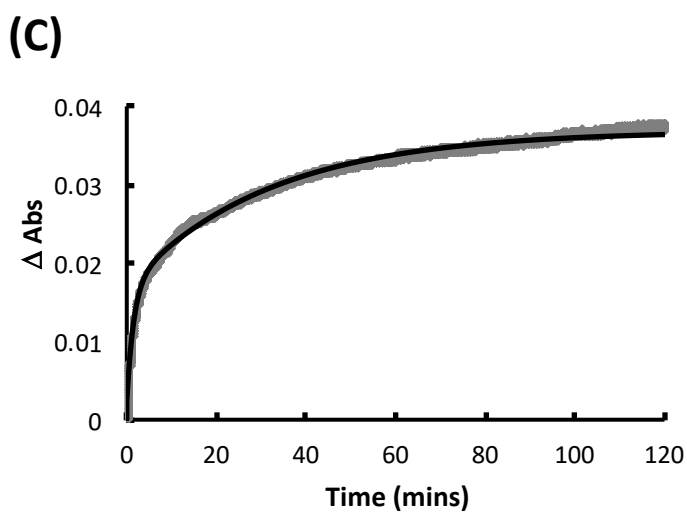
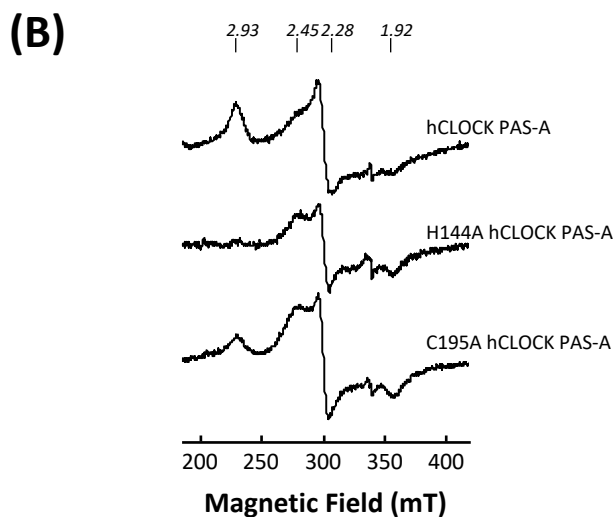
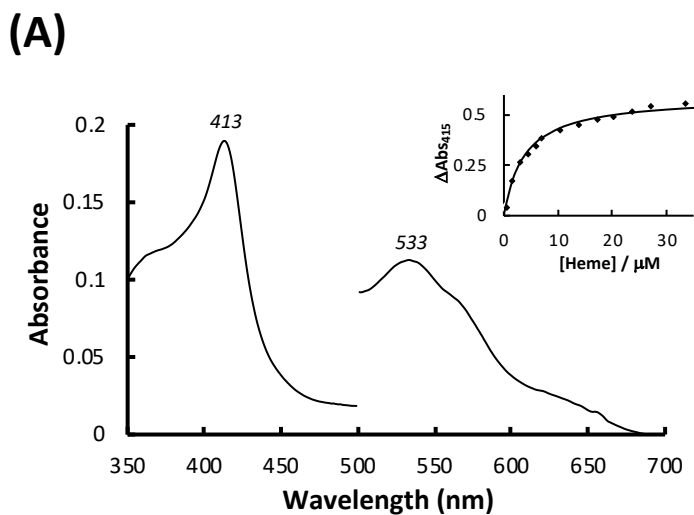


(B)

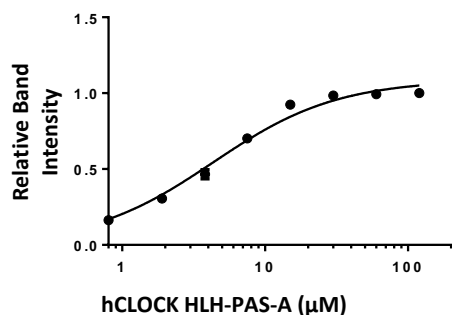


(C)





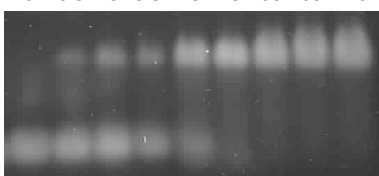
(A)



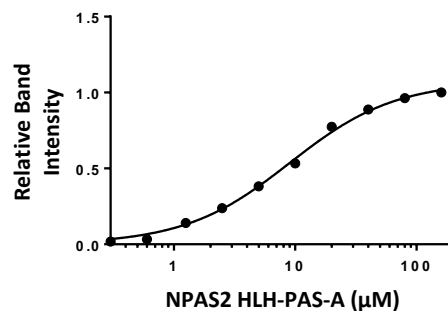
[CLOCK] / μM 0 0.8 1.9 3.8 7.5 15 30 60 120

CLOCK + DNA

free DNA



(B)



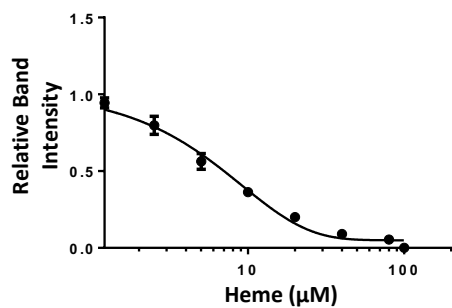
[NPAS2] / μM 0 0.3 0.6 1.2 2.5 5 10 20 40 80 160

NPAS2 + DNA

free DNA



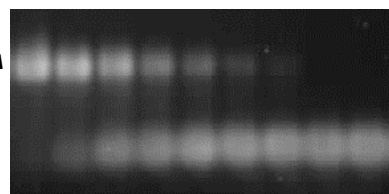
(C)



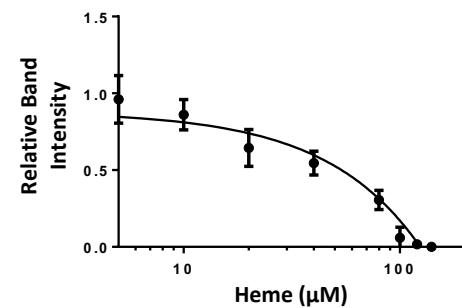
[Heme] / μM 0 1.2 2.5 5 10 20 40 80 100

CLOCK + DNA

free DNA



(D)



Heme / μM 0 5 10 20 40 80 100 120 140

NPAS2 + DNA

free DNA

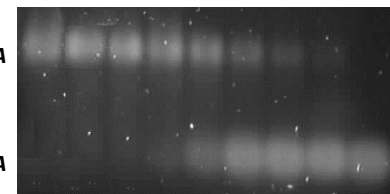
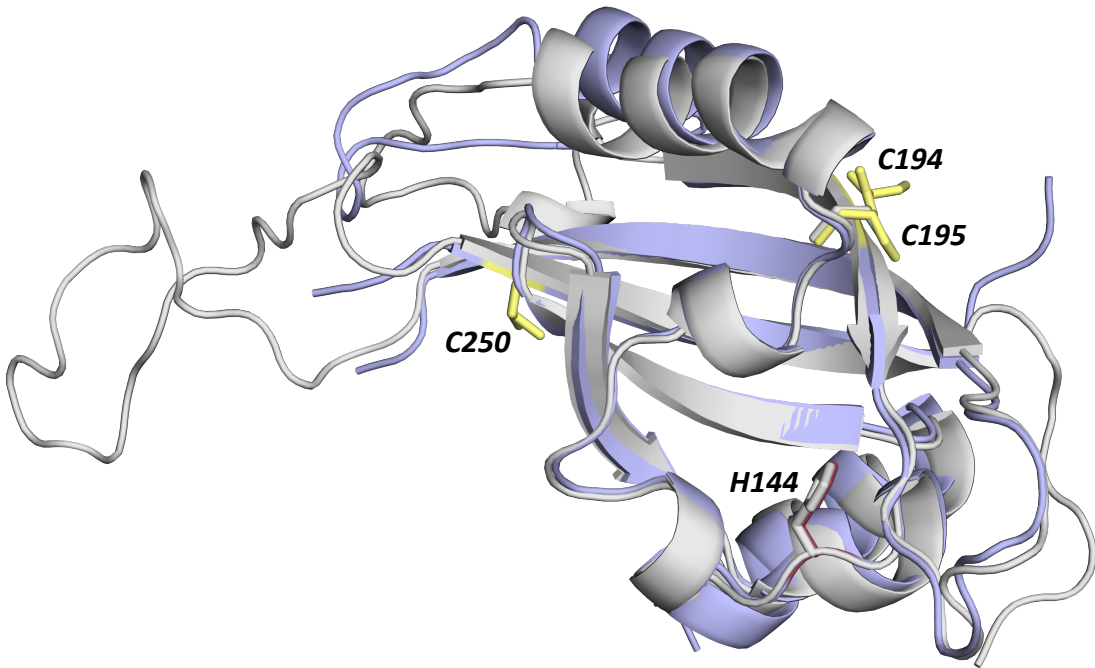


**Figure 6** Freeman *et al*



Supplementary Information for

**HEME BINDING TO HUMAN CLOCK AFFECTS INTERACTION WITH THE E-BOX**

Samuel L. Freeman<sup>1</sup>, Hanna Kwon<sup>1</sup>, Nicola Portolano<sup>2</sup>, Gary Parkin<sup>2</sup>, Umakhanth Venkatraman Girija<sup>2</sup>, Jaswir Basran<sup>2</sup>, Alistair J. Fielding<sup>4</sup>, Louise Fairall<sup>5</sup>, Dimitri A. Svistuneko<sup>3</sup>, Peter C. E. Moody<sup>3</sup>, John W. R. Schwabe<sup>3</sup>, Charalambos P. Kyriacou<sup>6</sup> and Emma L. Raven<sup>1\*</sup>

Corresponding author: Emma Raven  
Email: [emma.raven@bristol.ac.uk](mailto:emma.raven@bristol.ac.uk)

**This PDF file includes:**

Supplementary text  
Figures S1 to S8  
SI References

**Supplementary Information Text**

**Materials and Methods**

*Cloning and mutagenesis.* Constructs of human CLOCK (hCLOCK) were prepared from appropriate cDNA clones (Origene, Maryland, USA) by PCR and/or mutagenesis. Cloning into pLEICS expression vectors was performed by Dr. Xiaowen Yang at the PROTEX cloning and protein expression facility at the University of Leicester using a BD In-Fusion™ kit. Cloning into pOPINRSE expression vector was done at the Oxford Protein Production Facility. The following constructs were prepared: hCLOCK PAS-A, hCLOCK HLH-PAS-A and hCLOCK PAS-B, Fig. S1. Schematic details of these constructs and expression vectors are given in Figures 1 and S1. For controls in gel shift experiments, related constructs of human NPAS2 were also prepared (Fig. S2).

*Expression and purification.* All of the CLOCK constructs (PAS-A, HLH-PAS-A and PAS-B) produced soluble protein when overexpressed in *E. coli* and were purified in their apo-forms. The expression and purification protocols were thus the same for all of these constructs; yields ranged from 1-4 mg per liter of culture.

*E. coli* Rosetta 2(DE3) cells were transformed with the relevant construct and grown in 2xYT media with 30 µg/mL kanamycin at 37°C to an OD<sub>600</sub> of 0.6-0.8. Cells were induced by addition of IPTG (200 µM) and the cells incubated at 18 °C overnight. Cells were harvested by centrifugation at 5,500 g for 20 minutes. Cell pellets were re-suspended in lysis buffer (50 mM potassium phosphate pH 8, 300 mM potassium chloride, 10 mM imidazole) containing a cOmplete, EDTA-free protease inhibitor cocktail (Roche), lysozyme (1 mg/ml), DNase I (10 µg/ml) and magnesium sulphate (20 mM). Cells were then lysed by sonication on ice at 8-10 microns amplitude for 30 seconds at a time, separated by 30 seconds intervals. Cell lysate was centrifuged at 38,700 g for 50 minutes and the supernatant was applied to a Ni-NTA column equilibrated with lysis buffer. The column was washed with 300 ml wash buffer (50 mM potassium chloride pH 8, 300 mM potassium chloride, 20 mM imidazole) and the protein eluted using 0.1 M EDTA pH 8.0. Millipore centrifugation devices were used to exchange the protein into 50 mM potassium phosphate, 50 mM potassium chloride pH 8 buffer. Concentrated protein was incubated at 4 °C with TEV protease overnight to remove the 6xHis-tag. The protein was then passed through a Ni-NTA column using wash buffer and loaded onto a Superdex75 16/60 gel filtration column equilibrated with 50 mM Tris, 50 mM potassium chloride, pH 7.5.

All proteins were expressed and purified in their apo-forms (*i.e.* without heme included). Reconstitution with heme was carried out by dissolving an arbitrary amount of hemin (typically 30-40 mg) into 100 µl of 0.1 M NaOH. The solution was then diluted into 900 µl of 50 mM Tris, 50 mM potassium chloride, pH 7.5 buffer, and centrifuged at 20,000 g for 2 minutes. The supernatant was retained and centrifuged a second time at 20,000 g for 2 minutes. The insoluble pellet was discarded and 5 µl of soluble heme was further diluted into 1.0 ml of 50 mM Tris, 50 mM potassium chloride, pH 7.5 in order to determine its concentration ( $\epsilon_{385} = 58.44 \text{ mM}^{-1} \text{ cm}^{-1}$ ). This heme solution was added to the relevant protein solutions.

All purified proteins were assessed using SDS-PAGE, and by tryptic digestion followed by MALDI-ToF mass spectrometry analysis.

*Preparation of protein derivatives.* All absorbance spectra were measured using a Varian Cary 300 Bio UV-visible spectrophotometer (25.0 °C). Ferrous heme spectra were generated by addition of sodium dithionite to ferric protein samples. The ferrous-oxy and ferrous-CO derivatives were generated by direct bubbling of O<sub>2</sub> and CO gases, respectively, through dithionite-reduced samples. Binding constants for binding of heme to samples of apo-protein were determined according to (1). Modification of apo-CLOCK hCLOCK PAS-A (30 µM, in 50mM sodium phosphate pH 7.4) by reaction with Ellman's reagent (5,5'-dithiobis-(2-nitrobenzoic acid), DTNB) (3 mM final concentration) for 10 minutes at room temperature led to visible change in colour (to pale yellow) as the reaction proceeded. Excess DTNB and TNB were removed using a desalting column (GE Healthcare) which was equilibrated with 50 mM sodium phosphate pH 7.4 buffer.

*Crystallisation of hCLOCK PAS-A.* The holo-protein was purified as described above, with a final Superdex 75 column to exchange the protein solution into 20 mM Tris-HCl, 150 mM NaCl pH 7.5. The protein was concentrated to 13 mg/ml and crystals were grown using the hanging drop method

using a TTP Labtech Mosquito robot. Crystallisation of hCLOCK PAS-A in the apo- (heme free) form occurred from 2  $\mu$ L of protein solution and 2  $\mu$ L of reservoir solution (0.1 M MgSO<sub>4</sub>, 20% PEG 3,350, 20 mM MES pH 6.5). Irregular, plate-like crystals of the apo-protein grew to their maximum size within a week at room temperature. Soaking of apo-crystals in a solution of heme (over a range of concentrations) and co-crystallisation of holo-hCLOCK with heme were attempted, but did not lead to formation of crystals of the holo-protein. Crystals of apo-protein were soaked in a cryoprotectant solution consisting of the reservoir solution plus 10% glycerol and then flash frozen in liquid nitrogen prior to data collection. Data collection was carried out at the University of Leicester home-source. The data sets were collected at 100 K using CuK $\alpha$  radiation ( $\lambda = 1.5418$  Å) from a Rigaku MicroMax 007HF generator on a Rigaku Saturn 944+ detector. Data were indexed using iMOSFLM and then scaled and merged using AIMLESS as part of the CCP4 suite (2, 3). The protein crystallised as a homodimer with one monomer per asymmetric unit. The crystals belong to the I2 space group with unit cell dimensions of a = 46.0 Å b = 45.4 Å and c = 75.7 Å. Data collection and refinements statistics are shown in Table S1. The structure was determined by molecular replacement using the mouse CLOCK structure (PDB code: 4F3L) as the search model in Phaser (4) and refined with REFMAC (5) and COOT (6). Electron density of the polypeptide around H144 is shown in Fig. S3D.

**EPR spectra.** Protein samples (75-100  $\mu$ M) were prepared in 50 mM Tris/HCl buffer at pH 7.0 and flash frozen into 4 mm quartz EPR tubes. Continuous-wave (CW) electron paramagnetic resonance (EPR) spectra at 9 GHz were recorded using a Bruker EMX spectrometer. The spectrometer was equipped with a super high sensitivity probe head and a liquid helium cryostat (Oxford Instruments). Typical spectra were recorded under non-saturating conditions at 20 K, 7 G modulation amplitude, 100 kHz modulation frequency, 0.05 mW microwave power and 10 scans.

**Kinetic measurements.** Heme dissociation kinetics were measured using a Varian Cary 300 Bio UV-visible spectrophotometer (25.0 °C) (7). Samples of holo-hCLOCK (1  $\mu$ M, 50 mM potassium phosphate pH 7.0 containing 50 mM potassium chloride) were reacted with an excess concentration of apo-H64Y/V68F sperm whale myoglobin (80  $\mu$ M). The H64Y/V68F variant has a high affinity for heme and transfer of heme from holo-protein to apo- H64Y/V68F is monitored at 412 nm (7). Reported first order rate constants ( $k_{\text{diss}}$ , s<sup>-1</sup>) are an average of 2-4 determinations on different protein samples.

Pseudo-first order rate constants ( $k_{\text{CO}}$ , s<sup>-1</sup>) for binding of CO to hCLOCK (2  $\mu$ M) were also determined by stopped flow. Solutions of CO at fixed concentrations were prepared by anaerobic dilution of a CO-saturated buffer (50 mM potassium phosphate containing 50 mM potassium chloride, pH 7.0, 25.0 °C).

**Electrophoretic Mobility Shift Assays.** Samples containing double dilutions of protein ( $\leq 160$   $\mu$ M), double stranded E-Box DNA (2  $\mu$ M), 5% glycerol, and any additional ligands (e.g. heme) were prepared in 10 mM Tris/HCl containing 50 mM sodium chloride, pH 8.0. A 10  $\mu$ M double stranded E-Box DNA stock solution was prepared by combining equal volumes of 10  $\mu$ M 5'-GAGGGCGCCACGTGAGAGGCCT-3' primer and 10  $\mu$ M 5'-TAGGCCTCTCACGTGGC GCCCT-3' primer in 10 mM Tris containing 0.1 mM EDTA and 50 mM sodium chloride, pH 8.0, and stored at -20 °C. Samples were loaded on to a 0.7% agarose gel and separated by electrophoresis at 30 mA for 40 minutes. Gels were stained by soaking in 2.5  $\mu$ g/ml ethidium bromide in 0.5 x TB buffer for 15 minutes, followed by destaining for 15 minutes in deionised water. UV light was used to visualise ethidium bromide bound to DNA and the intensity of the bands was quantified using Image J (NIH and LOCI, University of Wisconsin) software. The ratio of bound to unbound DNA was used (yielding units of relative band intensity) with the band intensity of the protein-free sample taken as a reference.

## Human CLOCK

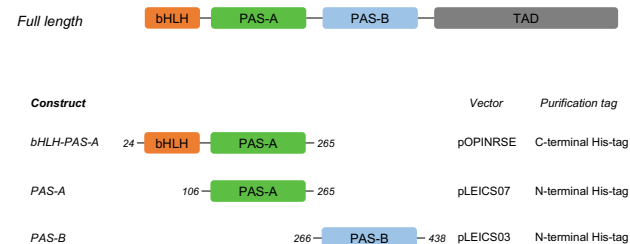


**Fig. S1.** Schematic figure showing the domains of the human CLOCK proteins studied in this work. The individual constructs along with details of the vector and purification tag are shown beneath each protein heading.

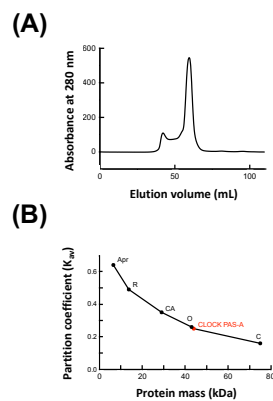


**Fig. S2.** Gel filtration of hCLOCK PAS-A using a Superdex 75 16/60 gel filtration column. (A) A typical elution profile. (B) Calibration curve of hCLOCK PAS-A elution plotted with protein standards.  $K_{av} = (V_e - V_0)/(V_c - V_0)$ , where  $V_e$ ,  $V_0$  and  $V_c$  are the protein elution volume, the void volume of the column and the geometric column volume, respectively. The standards are abbreviated as follows C: Conalbumin (75 kDa); O: Ovalbumin (43 kDa); CA: Carbonic Anhydrase (29 kDa); R: Ribonuclease A (13.7 kDa); Apr: Aprotinin (6.5 kDa). hCLOCK PAS-A elutes at 60 mL consistent with the enzyme being a dimer.

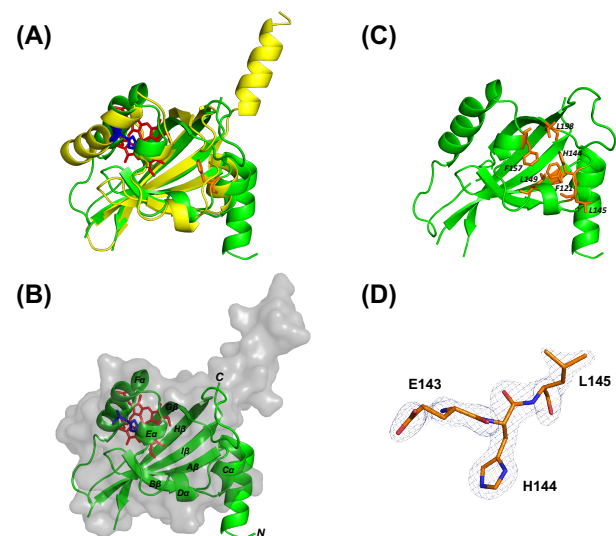


**Fig. S3.** (A) The structure of hCLOCK PAS-A (green) superimposed with the structure of FixL (yellow, PDB 1DRM). The RMSD of the two structures is 2.4 Å over 273 atoms. The heme of FixL is shown in red with its proximal histidine in blue and His144 of hCLOCK is shown in orange. This orientation is looking directly at the hydrophobic pocket which contains the heme group in FixL. (B) Space-filling representation of the same overlay, with the CLOCK structure shown in green overlaid onto a space filling image of FixL. The individual helices and sheets are labelled in green for hCLOCK, including the  $C\alpha$  helix (see Discussion). (C) The same cartoon representation of hCLOCK PAS-A as in (B) with the hydrophobic residues that form the mouth of the heme binding cavity shown as orange sticks and labelled accordingly. In this figure, the orientation is rotated slightly compared to (A) and (B) so that the position of His144 in the figure is not obscured by Phe121. (D) Local electron density of residues E143, H144 and L145 of hCLOCK ( $2F_o - F_c$  contoured at  $0.4 \text{ e}/\text{Å}^3$ ).



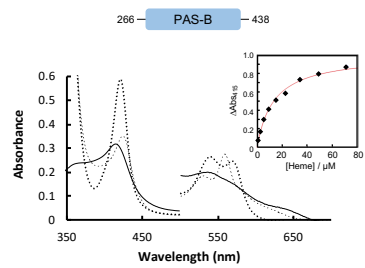


**Fig. S6.** Expression of hCLOCK PAS-B (construct shown in blue) gave a soluble protein (see methods). The UV-visible absorption spectrum shows that heme binds to hCLOCK PAS-B in the ferric (solid line), ferrous (dashed line) and ferrous-CO (dotted line) derivatives (50 mM phosphate and 50 mM potassium chloride buffer at pH 7.0). Inset shows  $\Delta$ Abs at 415nm (obtained from difference spectra at various heme concentrations) as a function of heme concentration and fitted to a 1:1 binding event.

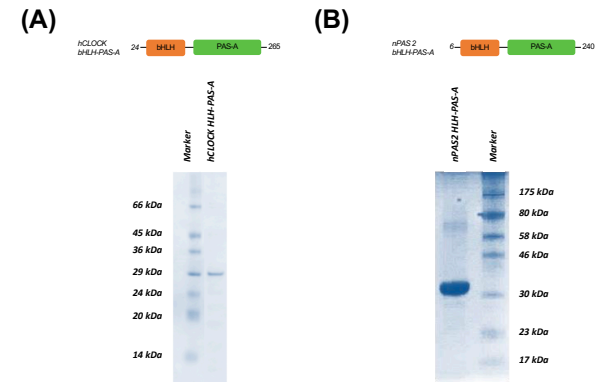


**Fig. S7.** (A) SDS-PAGE of purified hCLOCK HLH/PAS-A (amino acids 24 to 265 with a C-terminal 6 x His-tag, Fig. 2, 28.7 kDa) after expression in *E. coli* and elution from a Ni-NTA column. (B) SDS-PAGE of purified hNPAS2 HLH/PAS-A (32 kDa). The protein expressed in *E. coli* (amino acids 6 to 240 with an N-terminal 6 x His-tag and S-tag followed by a TEV cleavage site, Fig. S2). The protein was purified using Ni-NTA and FPLC gel filtration columns (see Methods).

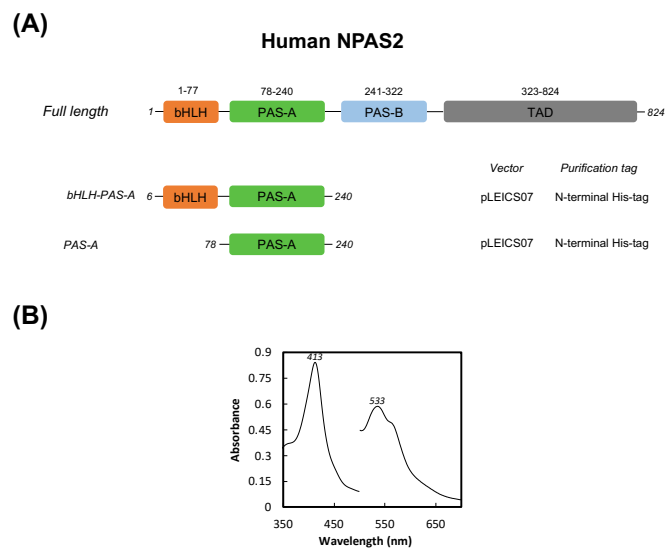


**Fig. S8.** (A) Schematic figure showing the domains of human NPAS2 (top) along with the NPAS2 constructs used in this work. NPAS2 constructs were overexpressed in *E. Coli* BL21(DE3) cells and purified in their apo-forms, following the procedure for expression and purification used for CLOCK PAS-A. A typical yield of 1 mg/L of soluble protein was obtained. (B) UV-visible spectrum of heme bound to ferric NPAS2 PAS-A ( $K_D = 0.75 \pm 0.04 \mu\text{M}$ ). Absorbance values between 500-700 nm have been magnified by a factor of five.

**Table S1.** Data collection and refinement statistics for hCLOCK PAS-A (PDB code 6QPJ). Values in parentheses are for high resolution shells

Data Collection	
Resolution (Å)	25.0-2.30 (2.40-2.30)
Total Measured Reflections	22826
Unique reflections	6784
Completeness (%)	98.4 (86.5)
Redundancy	3.4 (2.6)
$I/\sigma(I)$	10.8 (2.8)
Unit cell dimensions	a = 46.0 Å b = 45.4 Å and c = 75.7 Å
Space group	I2
$R_{\text{merge}}$	0.07 (0.32)
No. of monomers per asymmetric unit	1
Refinement	
Resolution (Å)	25.0-2.30
$R_{\text{work}}/R_{\text{free}}$	0.18/0.24
r.m.s.d. bond (Å)/angle (°)	0.008/1.28
$B$ -factor analysis (Å <sup>2</sup> )	
Protein	32.0
Water	35.5
Ramachandran analysis	
Most favoured (%)	96.12
Allowed (%)	3.1
Disallowed (%)	0.79

## References

1. Kapetanaki SM, *et al.* (2018) A mechanism for CO regulation of ion channels. *Nat Commun* 9(1):907.
2. Leslie AG (2006) The integration of macromolecular diffraction data. *Acta Crystallogr D Biol Crystallogr* 62(Pt 1):48-57.
3. Winn MD, *et al.* (2011) Overview of the CCP4 suite and current developments. *Acta Crystallographica Section D* 67(4):235-242.
4. McCoy AJ (2007) Solving structures of protein complexes by molecular replacement with Phaser. *Acta Crystallogr D* 63(Pt 1):32-41.
5. Murshudov GN, Vagin AA, & Dodson EJ (1997) Refinement of macromolecular structures by the maximum-likelihood method. *Acta Crystallogr D Biol Crystallogr* 53(Pt 3):240-255.
6. Emsley P & Cowtan K (2004) Coot: Model-Building Tools for Molecular Graphics. *Acta Crystallographica* D60:2126-2132.
7. Hargrove MS, *et al.* (1994) His64(E7)-->Tyr apomyoglobin as a reagent for measuring rates of heme dissociation. *J Biol Chem* 269(6):4207-4214.